Active coherent beam combining of 1.55μm pulsed fiber lasers based on intrapulse sampling

Zhen Liu[1,2], Yongke Zhang[1], Qihao Shen[1,2]*, Xingkai He[1,2], Dingfu Zhou[1,2], Liangyou Duan[1,2], Siyin Liu[1,2]

[1]Southwest Institute of Technical Physics, Chengdu, 610041, China

[2]Lidar and Device laboratory of Sichuan, Chengdu, 610041, China

Received Month X, XXXX; accepted Month X, XXXX; posted online Month X, XXXX

This letter presents an active coherent beam combining (CBC) of a pulsed laser based on sampling the intrapulse evaluation function. By precisely controlling trigger sequence of an analog-to-digital converter (ADC), the fixed time point of the pulse light is sampled as evaluation function for CBC. The active CBC of two fiber amplifiers with a 500 ns pulse width and 10 kHz repetition rate is experimentally demonstrated by applying a hill-climbing algorithm. The residual phase error is approximately λ/27. A coherent Doppler wind lidar (CDWL) based on CBC light source is verified. The experimental results verify the feasibility of using the pulsed CBC to improve the pulse energy of a CDWL without degrading performance.

Keywords: Single-frequency fiber laser; pulsed coherent beam combining; coherent Doppler lidar; active phase control
DOI: 10.3788/COLXXXXXX.XXXXXX.

1. Introduction.

CDWLs have been widely applied in aviation security[1], climate modeling[2], wind farm project optimization, and other fields. 1.55 μm single-frequency fiber lasers with low noise, narrow linewidth, high beam quality, and high integration have become primary light sources for CDWLs. For a high single-pulse energy output of single-frequency pulsed fiber lasers, the main oscillating power amplifier (MOPA) structure using erbium–ytterbium-doped fibers is well adapted[3]. However, fiber amplifiers easily excite nonlinear effects owing to their small mode field area and high power density, and stimulated Brillouin scattering (SBS) is a nonlinear process with the lowest threshold because of approximately kHz linewidth of the light source, limiting the peak power of the output lasers[4-6]. CBC allows the combination of the energy of serial fiber amplifiers and output light source while simultaneously maintaining the linewidth, beam quality, and polarization degree of the sub-beam. This is an important method to overcome the bottleneck of single-frequency pulsed fiber laser energy[7,8].

In a continuous CBC system, the phase compensation direction is determined by the sampling intensity value. However, the intensity modulation of the pulsed laser affects the judgment of the phase difference[9-11]. Therefore, extracting the phase difference between each sub-beam is a research focus for pulsed CBC systems. Currently, for low-repetition (< 100 kHz) pulsed CBC adopted in CDWL, the phase lock is mainly achieved using a low-power CW light leak. L. Lombard et al. realized a two-element CBC of nanosecond pulsed lasers with 10 kHz repetition rate by applying the dithering algorithm in 2013[7]. In 2013, Su et al. realized a two-element CBC of hundred-nanosecond pulsed lasers with a 5 kHz repetition rate at a combining efficiency of 89%[12]. Fan et al. simultaneously accomplished phase locking and tilt correction and realized a two-element CBC of pulsed fiber lasers with a repetition frequency of 15 kHz and pulse width of 100 ns at a combining efficiency of 95% via SPGD algorithm in 2023[13]. Nonetheless, the pulsed CBC system using a continuous wave as the beacon signal is complex. For CDWL, emission source with CW light results in additional optical noise and low signal-to-noise ratio.

This letter presents the active CBC of pulsed laser based on sampling the intrapulse evaluation function for CBC with low repetition, avoiding CW light leakage. Meanwhile, the pulsed CBC system based on intrapulse sampling is simpler than using a low-power CW light leak. Phase locking is accomplished by directly sampling a fixed time point of the pulsed light as the feedback signal of the active phase control evaluation function. The experimental results demonstrated that the pulsed CBC technology is applicable for improving pulse energy of a CDWL without degrading performance.

2. Principle and Method.

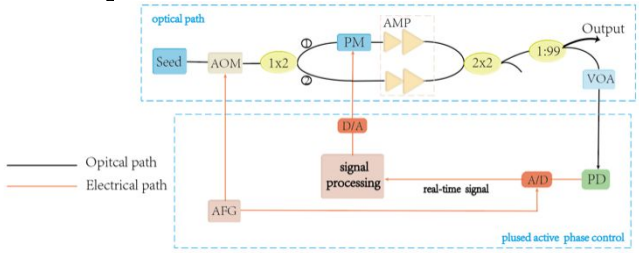

Fig1. Experimental setup for active pulsed coherent beam combining.

The experimental setup of the active pulsed CBC is shown in Fig.1, which includes part of the CBC optical path and pulsed active phase control. For the CBC optical path, a 1550nm DBR seed laser with power of 10mW is modulated using an acoustic-optic modulator (AOM) to produce 500 ns pulses at a repetition frequency of 10kHz. The output of the pulsed laser is then split into two arms using a 50/50 coupler. One arm is coupled to a phase modulator with a 4V half-wave voltage, which is controlled to achieve phase synchronization. The two arms are coupled to a two-stage fiber amplifier. The first stage is an Er-doped fiber amplifier, and the second stage is an ErYb co-doped fiber amplifier. The average laser power in two channel is 70 mW and single pulse energy is 7μJ. The

amplified outputs of the two laser channels are combined using a 2×2 coupler. Then the combined beam is split into two arms using a 1/99 splitter. The port with power of 99% as output arm and the 1% as feedback arm.

In pulsed active phase control, to generate the phase-control signal in the pulsed active phase controller, the feedback arm is attenuated to an appropriate range using an attenuator (VOA) and connected to a photodetector (PD). The intensity detected by PD is defined as evaluation function J and will be used in the hill-climbing algorithm, which was employed to make the evaluation function J and the laser power of output beam to be maximum. The phase control processes are as follows:

(1) Set phase control voltage u, then obtain corresponding evaluation function J; Generate disturbance voltage $\pm\delta u$;

(2) Compared J with J_{th}. If $J > J_{th}$, keep phase control voltage unchanged and acquire real-time evaluation function to compare with J_{th}; If $J < J_{th}$, carry out (3) procedure;

(3) Set phase control voltage $u + \delta u$, then obtain corresponding evaluation function $J(u + \delta u)$;

(4) Compared $J(u + \delta u)$ with $J(u)$. If $J(u + \delta u) > J(u)$, apply the control voltages with the $+\delta u$ to the PM in next disturbances, return to (2) procedure; If $J(u + \delta u) < J(u)$, apply the control voltages with the $-\delta u$ to the PM in next disturbances, then obtain corresponding evaluation function $J(u - \delta u)$;

(5) Compared $J(u - \delta u)$ with $J(u)$. If $J(u - \delta u) > J(u)$, apply the control voltages with the $-\delta u$ to the PM in next disturbances; repeat procedure (2) to (5).

The above phase control processes require real-time acquisition of evaluation functions J. However, the signal light intensity cannot always be obtained using pulsed lasers. Therefore, the timing of the trigger acquisition is synchronized with the AOM driving signal to acquire the evaluation function J and achieve feedback control. The control timing diagram of the pulsed CBC is shown in Fig.2. By controlling the timing of the AOM driving and ADC trigger signal using an arbitrary function generator (AFG), the pulsed signal can be sampled at a fixed point of the pulse light to avoid sampling errors caused by the non-rectangular pulse waveform after the gain of the fiber amplifier. Since the pulse width is on the order of hundreds nanoseconds which need accurate sampling, the AFG and ADC with 2.5GHz sampling rate are used in Fig.1. Then phase control voltage is judge by hill-climbing algorithm. According to the hill-climbing phase control processes, the direction of voltage control is determined by comparing the evaluation function before and after applying the disturbance voltage. For the pulsed CBC, the comparison is the fixed point acquisition value of adjacent pulses.

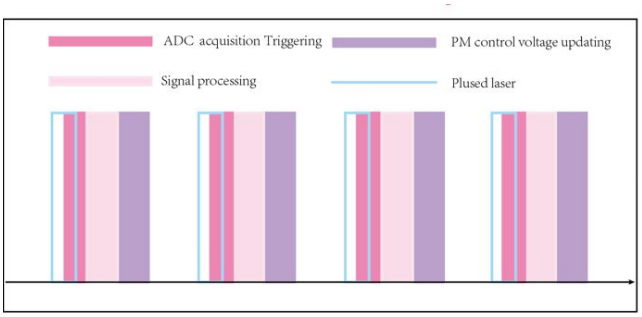

Fig2. Control timing diagram of pulsed CBC.

3. Results of pulsed coherent beam combining.

In the pulsed CBC system based on intrapulse sampling, two factors can introduce additional perturbations in the acquisition of the evaluation function J. Firstly, during the sub-beam amplification, pump disturbances, amplification of spontaneous emission and other factors can cause intensity noise, leading to instability in the sub-beam waveform. Secondly, the delay of electronic components limits the accuracy of sampling timing, and there will be errors in the acquisition of non-rectangular pulse waveforms. Before implementing the pulsed CBC, we sampled the intensity of the two pulsed sub-beams at the fixed time point to judge the effects of waveform instability and acquisition timing accuracy on J, as shown in Fig.3. The fixed time point is set at the flatter middle part of the pulse waveform. The fluctuation of the sampled values from the two sub-beams is less than 2%, and the disturbance to J is small compared to δu. Therefore, the influence on the phase control processes can be disregarded.

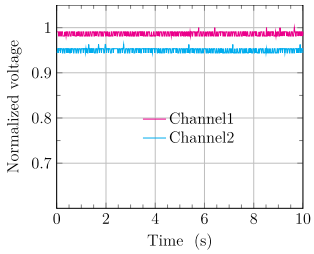

Fig3. Sampled intensity of the two pulsed sub-beams at the fixed time point.

The temporal profiles of the amplified and combined beams are shown in Fig.4. The consistency of the two fiber amplifiers is ensured to the maximum possible extent via the fabrication process, including the gain and fiber length (difference of less than 0.2 m). Therefore, the two pulsed lasers overlap in the time domain, and the combined pulse waveforms are consistent with those of the sub-beam. Figure 5 shows the changes in the power and normalized cost function J before and after loop closure. In the open-loop state, the output power fluctuates owing to the impact of vibration and thermal noise in the system, which results in a random phase jitter. By implementing a phase-locking feedback loop, the output power is stabilized at approximately 132 mW. A residual phase error of $\lambda/27$ is evaluated by the Equation. (1).

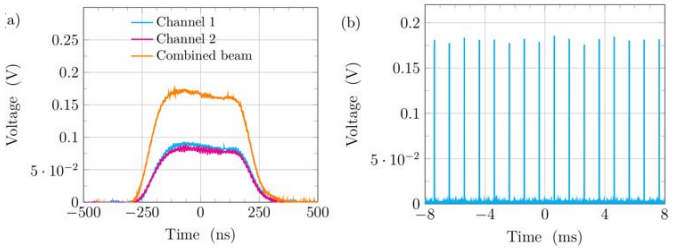

Fig4. Results.(a)Pulse shapes of two channel and combined beam in one cycle (b) pulse shape of combined beam in multicycle.

$$\varphi_{\mathrm{RMS}} = 2\sqrt{\frac{\Delta V_{\mathrm{RMS}}}{V_{\max}}}, \qquad (1)$$

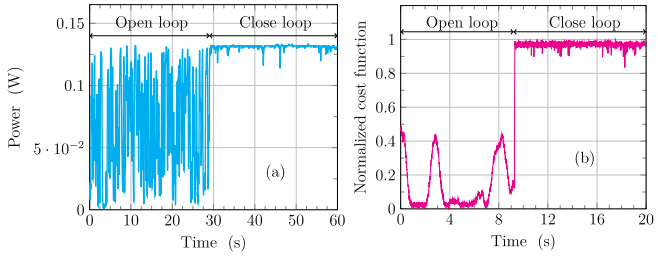

Fig5. Results. (a) output power in open loop and closed loop; (b) normalized cost function in open loop and closed loop

4. Application of pulsed coherent beam combining in CDWL.

Pulsed CBC can be applied to improve the emission energy. According to the lidar equation as shown in Eq. (2) [14],

$$\mathrm{P_{rec}} = \frac{\mathrm{E}\cdot\eta_{\mathrm{r}}\cdot\eta_{\mathrm{tran}}\cdot\beta\cdot\mathrm{c}\cdot A_{rec}\cdot\mathrm{T}^2}{2L^2} \propto \frac{\mathrm{E}}{L^2}, \qquad (2)$$

Where $\mathrm{P_{rec}}$ is the power of echo signal, E is the energy of the emission source, L is the detection range, η_r is the receiving efficiency, η_{trans} is the transmission efficiency, T is the single-way atmospheric transmittance, β is the atmospheric backscatter coefficient, α is atmospheric extinction coefficient, A_{rec} is the effective receiving area of the antenna, c is the speed of light. It can be seen that echo power is proportional to the emission energy. To verify the feasibility of pulsed CBC in CDWL, we compared the CDWL measurement results of the pulsed CBC with those of a conventional single-beam pulsed light source.

The setup of the CDWL based on pulsed CBC is shown in Fig.6. The circulator (CIR) separate transmitted pulsed laser and continuously optical atmospheric backscatter signal in opposite directions. The output light source is sent to the atmosphere via port 2 of the CIR. The transceiver system adopts an integrated configuration and uses a 100mm aperture telescope. The optical atmospheric backscatter signal will be received by the telescope. In the receiving system, the backscattered signal is mixed with local oscillator light using a 2X2 couple and beats on a balanced photodetector (BPD), realizing coherent detection.

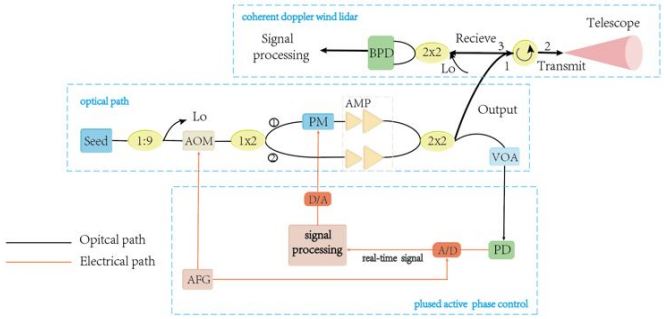

Fig6. The setup for coherent Doppler wind lidar based on pulsed coherent beam combining

Triple light source light sources are compared, including single-beam with 5.4 μJ (source A, listed in Table 1), single-beam with 10.8 μJ (source B, listed in Table 1), and two-beam CBC light source with 10.8 μJ (source C, listed in Table 1). Figure 7 shows the narrowband SNR of CDWL for three different light sources. Given the higher power, source C exhibits a 4dB higher SNR than source A. Meanwhile, the SNR of source C is comparable to that of source B.

Table 1. Parameter of light source

Source	Value	Illustrate
A	5.4μJ	Single-beam
B	10.8μJ	Single-beam
C	10.8μJ	Two-beam CBC

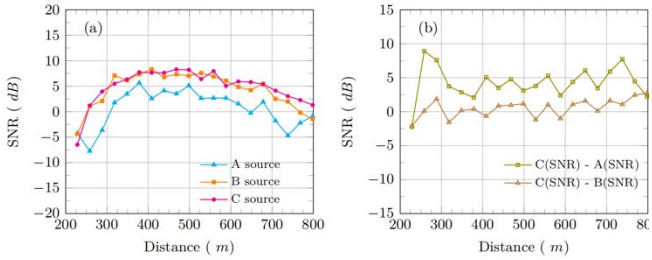

Fig7. Results of SNR. (a)average SNR; (b) SNR difference

Figure 8 shows the wind velocity profiles of the lidar for the three different light sources. Furthermore, Figure 8(a) denote source A. Figure 8(b) denote source B. Figure 8(c) denote source C. According to Eq. (2), the energy of a single pulse increases by a factor of two, and the detection range can be increased by $\sqrt{2}$ times. In Fig.8, the steady wind speed test distance range for pulsed CBC and single-beam light with 10.8 μJ is 1300 m, and single-beam light with 5.4 μJ is 950m. Compared to 5.4 μJ single-beam, the detection range of the CDWL using pulsed CBC is increased by 1.36 times. Overall, the CDWL performance of the CBC laser beam and single laser beam at equal energy is comparable, which verifies the feasibility of using the pulsed CBC to improve the pulse energy of a CDWL without degrading performance.

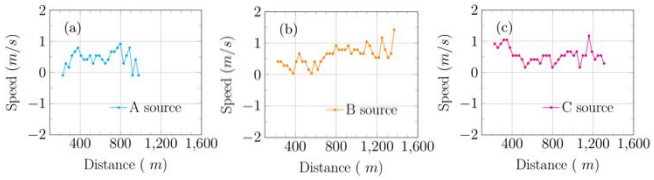

Fig8. Wind velocity profiles; (a) source A; (b) source B; (c)source C.

5. Discussion

The pulsed CBC based on intrapulse sampling requires accurate acquisition timing control. And narrower pulse width requires higher acquisition timing precision. Currently, electronic components, such as A/D chips, are limited to the GHz range, limiting the accuracy of acquisition timing to the nanoseconds level. Therefore, this scheme is more suitable for pulsed CBC systems with pulse width exceeding 100ns. Currently, CDWLs with all-fiber structured light sources and detection ability exceeding 10 km, the pulse widths are designied to 200ns ~ 1μs to achieve the requirement of sub-mJ level emission energy[15]. Therefore, the above emission source can serve as a sub-beam in an amplification array, compatible with the pulsed CBC technique based on intrapulse sampling. The fiber coupler with limited power handling is used as the beam combiner in Fig.1 and can be replaced by a polarization coherent beam combiner with higher power handling. Then, on the current output level of the 1.5μm single-frequency pulsed fiber laser, the multi-beam CBC can be achieved to break through output single pulse energy up to the mJ level and coherent detection at a longer distance.

6. Conclusion.

In conclusion, an active coherent beam combining of pulses laser based on sampling the intrapulse evaluation function is demonstrated. By precisely controlling trigger sequence of analog-to-digital converter(ADC), the fixed time point of the pulse light is sampled as the evaluation function. Then the hill climbing algorithm is applied to correct the phase errors. In experiment, the active CBC of two fiber amplifiers with a pulse width of 500 ns, 10kHz repetition rate of and $\lambda/27$ phase error has been achieved. Furthermore, the applicability of pulsed CBC in the system is verified. Experimental results show that the CDWL performance of the CBC laser beam and the single laser beam at equal energy are comparable, which verifies the feasibility of using the pulsed CBC to improve pulse energy of a CDWL without degrading performance. In the future work, the single-frequency pulse fiber laser based on the current output level can be combined by the pulsed CBC technology. This approach can overcome the limitations of output energy and provide a single-frequency laser source with higher pulse energy for lidar, atmospheric remote sensing, spectral analysis and other remote coherent detection fields with high spatio-temporal accuracy.

References

1. R, Stephan, I. Smalikho, and F. Kpp, "**Characterization of aircraft wake vortices by airborne coherent Doppler lidar**", Journal of Aircraft, 44(3): 799-805 (2007).
2. D. T. Michel, A. Dolfi-Bouteyre, D. Goular, et al, "**Onboard wake vortex localization with a coherent 1.5 μm Doppler LIDAR for aircraft in formation flight configuration**", Optics Express, 28(10): 14374-14385 (2020)
3. P. Wan, J. Liu, Lih-Mei. Yang, et al, "**Low repetition rate high energy 1.5 μm fiber laser**", Optics Letters, 19(19): 18067-18071(2011)
4. G. Canat, W. Renard, E. Lucas, et al, "**Eyesafe high peak power pulsed fiber lasers limited by fiber nonlinearity**", Optical Fiber Technology, 20(6): 678-687 (2014)
5. J. Hansryd, F. Dross, M. Westlund ,et al, "**Increase of the SBS threshold in a short highly nonlinear fiber by applying a temperature distribution**", Journal of Lightwave Technology, 19(11): 1691-1697 (2001)
6. L. V. Kotov, M. E. Likhachev, M. M. Bubnov, et al, "**Record-peak-power all-fiber single-frequency 1550 nm laser** ", Laser Physics Letters, 11(9) (2014)
7. L. Lombard, A. Azarian, K. Cadoret, et al,"**Coherent beam combination of narrow-linewidth 1.5 μm fiber amplifiers in a long-pulse regime** ", Optics Letters, 36(4): 523-525(2011)
8. L. Lombard, M. Valla, C. Planchat, et al, "**Eyesafe coherent detection wind lidar based on a beam-combined pulsed laser source** ", Optics Letters, 40(6): 1030-1033(2015)
9. P. Ma, P. Zhou, Y. Ma, et al. "**Coherent polarization beam combining of four fiber amplifiers in 100 ns pulsed-regime**", Optical and Laser Technology, 47: 336-340(2013).
10. F. Guichard, M. Hanna , L. Lombard, et al, "**Two-channel pulse synthesis to overcome gain narrowing in femtosecond fiber amplifiers**", Optics Letters, 38(24): 5430-5433(2013)
11. J. Zhang, J. Cao, Q. Hao, et al, "**Window filtering algorithm for a low repetition rate pulsed laser coherent combination system**", Applied Optics, 61(28): 8484-8492(2022).
12. R. Su, P. Zhou, X. Wang, et al, "**Actively Coherent Beam Combining of Two Single-Frequency 1083 nmnNanosecond Fiber Amplifiers in Low-Repetition-Rate**", IEEE Photonics Technology Letters, 25(15): 1485-1487(2013)
13. F. Zou, J Zuo, C. Geng, et al, "**Indirectly coherent beam combining of pulsed lasers based on active control of continuous carrier**", Optical Engineering, 60(6)(2021),
14. F, Takashi, F, Tetsuofukuch, **Laser Remote Sensing**(2005),.
15. R. William, G. Didier, V. Matthieu, et al. "**Beyond 10 km range wind-speed measurement with a 1.5 μm all-fiber laser source**" //proceedings of the 2014 Conference on Lasers and Electro-Optics (CLEO) -Laser Science to Photonic Applications, 2014.

Funding Sources. This work was supported supported by the Foundation of Lidar and Device Laboratory， Sichuan Province， China， the basic military research institutes steadily support special projects

Fujii, Takashi (EDT